Pure Rotational Spectrum and Structure of Platinum Monocarbonyl, PtCO

Corey J. Evans[†] and Michael C. L. Gerry*

Department of Chemistry, The University of British Columbia, 2036 Main Mall, Vancouver, British Columbia, Canada V6T 1Z1

Received: June 12, 2001; In Final Form: August 17, 2001

The pure rotational spectrum of platinum monocarbonyl, PtCO, has been measured between 6500 and 20 000 MHz, using a cavity pulsed jet Fourier transform microwave spectrometer. The molecules were prepared by laser ablation of Pt in the presence of CO contained in the Ar backing gas of the jet. Spectra of nine isotopic species have been measured and have been used to determine the molecular geometry. The centrifugal distortion constants agree well with those calculated from a literature force field. The ^{195}Pt nuclear spin−rotation constant has been used to estimate the ^{195}Pt shielding and its span.

1. Introduction

Platinum is an important metal, largely because of its catalysis properties. In particular, it finds widespread use in automobile catalytic converters, whose purpose is to remove CO, among other things, from the automobile exhaust. Poisoning of Pt electrodes by CO is of major concern in fuel cell technology (see, for example, refs 1 and 2). The adsorption of CO on Pt surfaces is also of great importance as a prototype for chemisorption in surface science; the simplest model of this is PtCO. Because the experimental evidence for PtCO consists only of matrix-isolation infrared studies,[3−5] there is no experimental geometry. On the other hand, there have been several ab initio studies over the past 20 years.[4−14] All these studies show PtCO to be linear, with a $^1\Sigma^+$ ground state. However, predicted geometries have varied widely, with the Pt−C distance varying from 1.71 to 2.07 Å over the various calculations. An experimental measurement of the geometry has clearly been needed.

Recently, we have measured using Fourier transform microwave (FTMW) spectroscopy the rotational spectra of two series of coinage metal halide complexes, namely noble gas metal halides, Ng−MX (Ng = Ar, Kr; M = Cu, Ag, Au; X = F, Cl, Br)[15−19] and carbonylmetal halides OC−MX (M = Cu, Ag, Au; X = F, Cl, Br).[20,21] The spectra, particularly of the carbonyls, were obtained with relative ease. Because the metals are all nominally in the +1 oxidation state, with which Pt(0) is isoelectronic, PtCO was thought to be a promising candidate to investigate by an analogous method.

In this paper, we report the detection and measurement of the pure rotational spectrum of PtCO. This is the first gas phase study of the molecule. From the spectrum, we have determined the rotational constants and centrifugal distortion constants and for the isotopomers containing ^{195}Pt, the nuclear spin−rotation coupling constants. The bond lengths have been calculated by several methods. The ^{195}Pt shielding and its span have been estimated.

* To whom correspondence should be addressed. Fax: +1 (604) 822-2847. Phone: (604) 822-2464. E-mail: mgerry@chem.ubc.ca.

[†] Present address: Department of Chemistry, University of Kentucky, Lexington, KY 40506-055, USA.

2. Experimental Procedure

The rotational spectrum of PtCO has been measured using Balle−Flygare type[22] cavity pulsed jet FTMW spectrometers, coupled to a laser ablation system. Because details of these instruments have been previously published,[23,24] only a brief description will be given here. At their heart is a Fabry−Perot cavity consisting of two aluminum spherical mirrors of diameter 28 cm, radius of curvature 38.4 cm and separation of ∼30 cm. One of the mirrors is fixed, whereas the other is used to tune the cavity to the desired polarization frequency.

A pulsed supersonic jet of noble gas (usually Ar), seeded with the sample gas, is injected into the cavity via a General valve Series 9 pulsed nozzle, mounted slightly off-center in the fixed mirror. Because the direction of the jet is parallel to the direction of propagation of the microwaves, all lines are doubled by the Doppler effect. The frequency range of the present experiments was 6−20 GHz. Frequency measurements were referenced to a Loran frequency standard accurate to 1 part in 10^{10}. Observed line widths were ∼7−10 kHz (FWHM). The estimated measurement uncertainties were ±1−2 kHz.

The laser ablation system has also been described earlier.[25] In it, a metal rod placed 5 mm from the orifice of the pulsed nozzle is irradiated using a Nd:YAG laser, as a gas pulse passes over its surface. In contrast to the experiments on the coinage metal complexes,[15−21] the best signals were obtained using the fundamental of the laser (1064 nm). The metal atoms in the plasma react with precursor gas(es) entrained in the backing gas. The gas pulse is then supersonically expanded into the cavity via a 5 mm diameter channel. The metal rod is continuously rotated and translated to expose a fresh surface of the metal to each laser pulse.

In the present experiments, the "rod" was a piece of Pt foil wrapped around a 4 mm diameter glass rod. The gas mixtures consisted of 1% CO in high purity Ar, at backing pressures of 6−7 bar. For the species containing ^{13}CO and C^{18}O the following artificially enriched samples were used: ^{13}CO (Cambridge Isotopes 99.9%, with ∼5% ^{13}C^{18}O) and C^{18}O (ICON, 28%).

3. Results and Analysis

The pure rotational spectrum of PtCO was initially predicted using bond lengths recently calculated ab initio by Chung et

10.1021/jp012215g CCC: $20.00
Published on Web 10/02/2001

TABLE 1: Observed Frequencies of PtCO (in MHz)

transition		^{194}PtCO		^{196}PtCO		^{198}PtCO		unc[b]
J'	J''	frequency	O−C[a]	frequency	O−C	frequency	O−C	(kHz)
1	0	6649.7173	−0.6	6641.6606	0.2	6633.7609	−1.7	±2
2	1	13299.4251	0.1	13283.3101	0.0	13267.5141	0.3	±1
3	2	19949.1101	0.0	19924.9387	0.0	19901.2421	−0.1	±1

transition		^{194}Pt^{13}CO		^{196}Pt^{13}CO		unc	^{194}PtC^{18}O		^{196}PtC^{18}O		unc
J'	J''	frequency	O−C	frequency	O−C	(kHz)	frequency	O−C	frequency	O−C	(kHz)
1	0	6558.4289	1.6	6550.2500	1.0	±2					
2	1	13116.8432	−1.3	13100.4875	−0.8	±2	12217.2327	0.0	12201.4778	0.0	±1
3	2	19675.2416	0.1	19650.7081	0.0	±1	18325.8274	0.0	18302.1920	0.0	±1

[a] Residuals (kHz). [b] Estimated uncertainties in the observed frequencies.

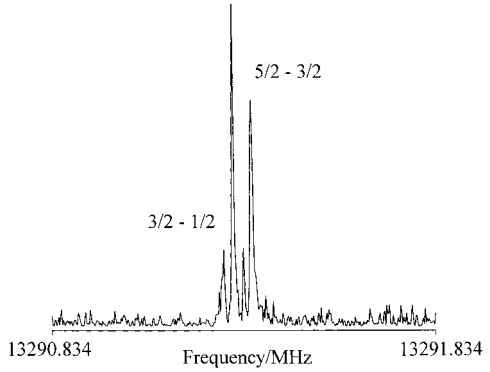

Figure 1. $J = 2-1$ transition of ^{195}Pt^{12}C^{16}O. Experimental conditions: 1% CO in Ar; 1000 averaging cycles; Pt foil on a glass rod; Pt ablated with 1064 nm radiation; 8 K transform.

al.[14] (relativistic Xα calculation). The uncertainties in the assumed bond lengths were taken to be ∼0.02 Å, which produced a search range of ∼300 MHz for the $J = 2-1$ transition. A strong line was found at 13 299.4 MHz, and further searching revealed a closely spaced doublet near 13 291.3 MHz. The latter is in Figure 1. Further lines were found at precise intervals of $2B$ (∼3300 MHz), to both lower and higher frequencies, thus confirming the observed lines were from a linear molecule. Platinum has six stable isotopes, of which four have significant abundance: ^{194}Pt (32.9%), ^{195}Pt (33.8%), ^{196}Pt (25.3%), ^{198}Pt (7.2%); all but ^{195}Pt have nuclear spin $I = 0$. The ^{195}Pt nucleus has $I = {}^1/_2$ and hence a magnetic moment, but not an electric quadrupole moment. It can thus undergo magnetic spin−rotation coupling whereby each rotational level except $J = 0$ is split into two. Thus, the doublet at 13291.3 MHz was assigned to ^{195}PtCO and the line at 13 299.4 MHz to ^{194}PtCO. A preliminary geometry was then determined and used to predict the spectra of ^{196}PtCO and ^{198}PtCO. They were found within 0.5 MHz of these predictions, and the assignments were thus confirmed. In total, lines were measured and assigned to the $J = 1-0$ to $3-2$ transitions of these four isotopomers. No lines of vibrationally excited molecules could be assigned despite extensive searches using both argon and neon as the backing gas.

Lines of isotopically enriched samples containing ^{13}CO and C^{18}O were measured and assigned to the sequence $J = 1-0$ to $3-2$ for ^{194}Pt^{13}CO, ^{195}Pt^{13}CO, and ^{196}Pt^{13}CO, as well as to the $J = 2-1$ and $3-2$ transitions of ^{194}PtC^{18}O and ^{196}PtC^{18}O. No hyperfine structure due to ^{13}C ($I = {}^1/_2$) was observed. The measured frequencies of all the isotopomers are given with their assignments in Tables 1 and 2. For the species containing ^{195}Pt the coupling scheme $\mathbf{J} + \mathbf{I_{Pt}} = \mathbf{F}$ was used.

TABLE 2: Observed Frequencies of ^{195}PtCO (in MHz)

transition				^{195}PtCO			^{195}Pt^{13}CO		
J'	F'	J''	F''	frequency	O−C[a]	unc[b] (kHz)	frequency	O−C	unc (kHz)
1	1/2	0	1/2	6645.6411	0.0	±2			
1	3/2	0	1/2	6645.6762	−1.2	±2	6554.3259	1.4	±2
2	3/2	1	1/2	13291.3084	0.7	±1	13108.6005	−1.7	±2
2	5/2	1	3/2	13291.3315	−0.4	±1	13108.6280	0.6	±2
3	5/2	2	3/2	19936.9399	−0.7	±1	19662.8879	0.5	±1
3	7/2	2	5/2	19936.9655	0.7	±1	19662.9122	−0.4	±1

[a] Residuals (kHz). [b] Estimated uncertainties in the observed frequencies.

The measured frequencies were fit using Pickett's global least squares program SPFIT,[26] to the constants in the Hamiltonian

$$\mathbf{H} = \mathbf{H}_{\text{rot}} + \mathbf{H}_{\text{spin-rot}} \tag{1}$$

where

$$\mathbf{H}_{\text{rot}} = B_0\mathbf{J}^2 - D_J\mathbf{J}^4 \tag{2}$$

$$\mathbf{H}_{\text{spin-rot}} = C_I(\text{Pt})\mathbf{I}_{(\text{Pt})}\cdot\mathbf{J} \tag{3}$$

The resulting molecular constants, including rotational constants, centrifugal distortion constants and, for the ^{195}Pt species, nuclear spin−rotation constants, are in Table 3.

4. Vibrational Wavenumbers

The distortion constants are related to the harmonic force field and vibrational wavenumbers of PtCO. Manceron et al.[4] have determined a complete harmonic force field for PtCO from their matrix infrared data. Distortion constants calculated from this force field are given in Table 4, in comparison with the experimental values. In general the agreement is excellent, within two standard deviation of the latter, thus verifying the force field and distortion constants.

An alternative approach is to evaluate the PtC stretching frequency using a diatomic approximation and the equation[27]

$$\omega \approx (4B_0^3/D_J)^{1/2} \tag{4}$$

This gives a value of ∼605 cm^{-1} for the main isotopomer, which agrees very reasonably with the experimental value of 580 cm^{-1}.[4] Evidently, the main contributor to the distortion constant is the stretching vibration.

5. Structure of PtCO

Because all the observed spectra were of molecules in the ground vibrational state, it was not possible to obtain directly the equilibrium (r_e) structure. Instead, geometries were deter-

TABLE 3: Molecular Constants of Nine Isotopomers of PtCO (in MHz)

parameters	^{194}PtCO	^{195}PtCO	^{196}PtCO	^{198}PtCO	^{194}Pt^{13}CO	^{195}Pt^{13}CO	^{196}Pt^{13}CO	^{194}PtC^{18}O	^{196}PtC^{18}O
B_0	3324.85989(43)[a]	3322.83356(31)	3320.83107(43)	3316.88224(43)	3279.21448(71)	3277.15667(57)	3275.12532(71)	3054.31106(47)	3050.37274(47)
$D_J \times 10^4$	4.55(28)	4.50(20)	4.42(28)	4.74(28)	4.20(42)	3.70(33)	4.06(42)	3.61(30)	4.12(30)
C_l(Pt) $\times 10^2$		2.420(87)				2.52(12)			

[a] Numbers in parentheses are one standard deviation in units of the last significant figure. They account both for deviations in least squares fits and for estimated measurement errors.

TABLE 4: Observed and Calculated[a] Centrifugal Distortion Constants (in MHz $\times 10^{-4}$) of PtCO

	^{194}PtCO	^{195}PtCO	^{196}PtCO	^{198}PtCO	^{194}Pt^{13}CO	^{195}Pt^{13}CO	^{196}Pt^{13}CO	^{194}PtC^{18}O	^{196}PtC^{18}O
obs	4.55(28)[b]	4.50(20)	4.42(28)	4.74(28)	4.20(42)	3.70(33)	4.06(42)	3.61(30)	4.12(30)
calcd[a]	4.73	4.72	4.72	4.71	4.64	4.64	4.63	3.53	3.92

[a] Calculated from the harmonic force field of Manceron et al.[4] [b] Uncertainties are one standard deviation in units of the last significant figure.

TABLE 5: Structure of PtCO[a]

method	r(Pt−C)	r(C−O)	comments
r_0	1.76249(42)	1.14662(59)	this work
$r_{I\epsilon}$	1.760145(24)	1.148136(21)	$\epsilon = 0.1487(14)$ amu Å^2, this work
$r_m^{(1)}$	1.759304(31)	1.147607(17)	$c = 0.0237(2)$ amu$^{1/2}$ Å, this work
$r_m^{(2)}$	1.76039(13)	1.14627(16)	$c = 0.0416(21)$ amu$^{1/2}$ Å $d = -0.0663(80)$ amu$^{1/2}$ Å^2, this work
r_z	1.76383(37)	1.14570(52)	
r_e (est.)	1.76046	1.14354	
		literature: ab initio	
r_e	1.74	1.16	DF, Xα(rel), ref 14
	1.78	1.16	DF, GC(rel), ref 14
	1.93	1.15	DF, Xα(non-rel), ref 14
r_e	1.753	1.160	MP2/LanL2DZ, ref 4
	1.757	1.159	MP2/Stoll, ref 4
	1.792	1.147	QCISD/Stoll, ref 4
	1.787	1.150	B3LYP/Stoll, ref 4
r_e	1.781	1.148	B3LYP, ref 5
		related molecules	
CO: r_e		1.128	ref 39
PtC: r_e	1.678		ref 40

[a] Bond distances in Å; numbers in parentheses are one standard deviation in units of the last significant figure.

mined by several methods. These included a ground-state effective (r_0) geometry, a fitted substitution geometry ($r_{I\epsilon}$), two mass-dependent ($r_m^{(1)}$ and $r_m^{(2)}$) geometries, and a ground-state average (r_z) geometry, from which was obtained an estimated r_e structure.

(i) Ground-State Effective (r_0) Geometry. This method ignores any vibrational contributions to the ground-state moments of inertia and rotational constants. The structural parameters were fit by least squares to the moments of inertia of various isotopomers using

$$I_0 = I_{\text{rigid}}(r_0) \tag{5}$$

where $I_{\text{rigid}}(r_0)$ is calculated from the structural parameters r_0 using rigid molecular formulas. The result is listed as the r_0 geometry in Table 5.

(ii) Fitted Substitution ($r_{I\epsilon}$) Geometry. In this method, the ground-state rotational constants are fit to[28]

$$I_0 = I_{\text{rigid}}(r_{I\epsilon}) + \epsilon \tag{6}$$

where ϵ is a vibration−rotation correction to I_0, assumed to be independent of isotopomer. This is the same assumption as is made in the conventional substitution (r_s) method,[29] in which a basis molecule is chosen and atomic positions are determined by making isotopic substitutions at each atom. Where principal moments of several isotopic species have been obtained (as in the present case), the resulting structures should be the same.

The result of an $r_{I\epsilon}$ fit to all measured principal moments of inertia is also in Table 5. Unsurprisingly, because ϵ compensates at least in part for vibration−rotation contributions, the bond lengths are an order of magnitude better determined than the r_0 values.

(iii) Mass Dependent $r_m^{(1)}$ and $r_m^{(2)}$ Geometries. These geometries attempt to account for the mass dependence of ϵ in eq 6 and thus should produce near-equilibrium geometries from the ground-state moments of inertia. For a linear triatomic molecule such as PtCO, they are obtained using the equation[30]

$$I_0 = I_m(r_m) + c(I_m)^{1/2} + d(m_1 m_2 m_3/\text{M})^{1/4} \tag{7}$$

where $I_m(r_m)$ is I_{rigid} using the r_m bond lengths, and c and d are constants. In an $r_m^{(1)}$ fit d is set to zero; in an $r_m^{(2)}$ fit both c and d are included as fit parameters. The results of both these fits are in Table 5.

Because its fit is to one constant not part of the moment of inertia, the $r_m^{(1)}$ method behaves like the $r_{I\epsilon}$ method in terms of uncertainties and correlations. The $r_m^{(2)}$ fit accounts in principle more completely for mass dependence, but the determined parameters are sometimes strongly correlated, especially when the molecule contains no atom near the center of mass;[30] this is the case here. An attempt was made to remove the correlation by fixing c to its $r_m^{(1)}$ value and re-fitting to d; this, however, produced an indeterminate value for d. Although they are strongly correlated, the $r_m^{(2)}$ values for both the PtC and CO bond lengths are smaller than the r_0 values, as normally expected in a diatomic approximation for a near-equilibrium structure. Following the results in ref 30, these are expected to be good approximations to the r_e values.

(iv) Ground-State Average (r_z) and Estimated Equilibrium (r_e) Geometries. The r_z geometry was calculated for ^{195}Pt^{12}C^{16}O, the most abundant isotopomer. Because the harmonic force field of ref 4 reproduced the distortion constants well, it was used to evaluate the harmonic contributions to the α-constants. These were subtracted from the experimental rotational constants to produce ground-state average (B_z) values. The r_z geometry was calculated by fitting to the B_z constants by least squares. The isotopic variations in the bond lengths were accounted for using[31,32]

$$\delta(r_z) = \frac{3}{2} a \delta\langle u^2 \rangle - \delta(K) \tag{8}$$

TABLE 6: Comparison of M−C and −CO Bond Lengths (in Å)

molecule	r(M−C)	r(C−O)	comments
OC−Pt	1.760	1.148	FTMW, this work ($r_{I\epsilon}$ structure)
OC−Ni	1.687	1.166	CCSD[T], ref 41
OC−Fe	1.727	1.160	FTMW, ref 42
OC−Ir	1.769	1.179	BP96, ref 43
OC−Os	1.795	1.148	MRSDCI, ref 44
OC−Ta	2.012	1.184	BP86, ref 45
OC−Hf	2.070	1.186	BP86, ref 46
OC−AuF	1.847	1.134	FTMW, ref 20 (r_0 structure)
OC−AuCl	1.883	1.132	FTMW, ref 20 ($r_{I\epsilon}$ structure)
OC−AuBr	1.892	1.132	FTMW, ref 20 ($r_{I\epsilon}$ structure)
OC−CuF	1.765	1.131	FTMW, ref 21 ($r_{I\epsilon}$ structure)
OC−CuCl	1.795	1.129	FMTW, ref 21 ($r_{I\epsilon}$ structure)
OC−CuBr	1.803	1.128	FTMW, ref 21 ($r_{I\epsilon}$ structure)
OC		1.128	r_e value, ref 39

The required zero-point mean square amplitudes, $\langle u_2 \rangle$, of the bonds and their perpendicular amplitude corrections, K, were obtained from the force field. The Morse parameter, a, for CO was obtained from tabulated values.[33] That of PtC was estimated from the force constants and dissociation energies in ref 4, using $k = 2D_e a^2$; the value used was 1.88 Å^{-1}. The resulting r_z bond lengths are also in Table 5, with the uncertainties arising from the least-squares fit.

An estimate of the equilibrium geometry was also calculated from the r_z geometry using[31,32]

$$r_e = r_z - \frac{3}{2} a\langle u^2 \rangle + K \tag{9}$$

This is also in Table 5. The uncertainties in the bond lengths, which are difficult to estimate, are probably similar to those of the r_z values. It is interesting that although the estimated r_e value for r(PtC) agrees well with the $r_m^{(2)}$ value, this is not the case for r(CO). The reason for the difference is not obvious, for both are expected to be good approximations to the true r_e. The dilemma will only be removed when a true equilibrium geometry is determined.

Also listed in Table 5 are several recent ab initio determined structures. The best agreement with r_0(PtC) was produced by the MP2/Stoll and MP2/LanL2DZ calculations of Manceron et al.[4] Chung et al. [14] have explicitly pointed out that relativistic effects must be taken into account in understanding the bonding, and the agreement of their relativistic calculations with experiment confirms this conclusion. It is interesting to note that Chung et al. have also predicted that relativistic effects will cause the PtC bond in PtCO to be shorter than the PdC bond in PdCO. Experiments are currently underway to examine this prediction.[34]

The derived geometry is compared with those of several related molecules in Table 6. The PtC bond is relatively short, roughly 0.1 Å shorter than the AuC bond in the carbonyl gold halides. In addition, the CO bond length in PtCO is greater than that in free CO and in all the carbonyl coinage metal halides. The bonding in PtCO is apparently easily rationalized in terms of the conventional bonding picture of transition metal carbonyls (σ-donation from CO to the metal plus π-back-donation to CO antibonding orbitals). This is not the case for the carbonyl coinage metal halides,[20,21] even though the coinage metals are in the +1 oxidation state and thus isoelectronic with Pt in PtCO.

6. ^{195}Pt Shielding Constant

Nuclear spin−rotation constants are strongly related to NMR shielding constants σ. They provide a valuable source of shielding constants in situations unfavorable in NMR experiments (e.g., for transient molecules or where quadrupole broadening is a factor). Spin-rotation constants give shieldings for isolated gas-phase molecules, eliminating the need to consider environmental (e.g., solvent) effects. Furthermore, the shieldings are determined directly, without the necessity of making comparisons with a standard.

Accordingly, the average shielding, σ, of ^{195}Pt in PtCO has been calculated from its spin−rotation constant C_I. Of the several ways of doing this, the one which probably gives the most information about the molecule is first to divide C_I into its nuclear and electronic contributions[35]

$$C_I = C_I(\text{nuc}) + C_I(\text{elec}) \tag{10}$$

The nuclear part C_I(nuc) depends only on the nuclear positions and is given for a linear molecule by

$$C_I(\text{nuc}) = -\left(\frac{2e\mu_N g_I B}{hc}\right)\sum_{i\neq A}\left(\frac{Z_i}{r_{Ai}}\right) \tag{11}$$

where e is the proton charge; μ_N is the nuclear magneton; g_I is the g-factor for the nucleus in question, A (=^{195}Pt in this case); B is the rotational constant; Z_i is the atomic number of nucleus $i \neq A$; r_{Ai} is the distance from nucleus A to nucleus i. This gives C_I(nuc) = −0.38 kHz, so consequently C_I(elec) = C_I − C_I(nuc) = 24.58 kHz.

This shielding is also divided into two contributions

$$\sigma = \sigma_\text{p} + \sigma_\text{d} \tag{12}$$

where σ_p and σ_d are the paramagnetic and diamagnetic parts, respectively. The paramagnetic part is proportional to C_I(elec)

$$\sigma_\text{p} = -\left(\frac{e\hbar}{6mc\mu_N g_I B}\right)C_I(\text{elec}) \tag{13}$$

$$= -\left(\frac{m_\text{p}}{3mg_I B}\right)C_I(\text{elec}) \tag{14}$$

where m and m_p are the masses of the electron and proton, repectively. From recent values of the fundamental constants,[36] if C_I is in kHz and B is in MHz, then σ_p in ppm is

$$\sigma_\text{p} = -612\,050.90(58)\left(\frac{C_I(\text{elec})}{g_I B}\right) \tag{15}$$

This gives σ_p = −3714(134) ppm for ^{195}Pt in PtCO. Finally, the diamagnetic part is calculated using

$$\sigma_\text{d} = \left(\frac{m_\text{p}}{3mg_I B}\right)C_I(\text{nuc}) + \sigma_\text{d}(\text{atom}) \tag{16}$$

in which σ_d(atom) is the free atom diamagnetic shielding, normally obtainable from tables.[37] Reference 37 gives this as 9366 ppm, making σ_d = 9424 ppm. The resulting value for σ is 5710 ppm.

The reliability of σ depends entirely on that of σ_d(atom). For light atoms the tabulated values of the latter[37] appear accurate. However, the estimates of σ_d(atom) do not take into account relativistic effects, which are considerable for Pt,[14] so the value obtained for σ must be viewed very cautiously. One should note, however, that the span of the shielding, which is a measure of

its asymmetry,[38] is independent of σ_d(atom) and should be reliable to within a few ppm. It is given by[38]

$$\Omega = \left(\frac{m_p}{2mg_IB}\right)C_I \qquad (17)$$

where the span, Ω, is defined by $\Omega = \sigma_{||} - \sigma_{\perp}$, with $\sigma_{||}$ and $\sigma_{\perp}$ being the components of the shielding tensor parallel and perpendicular to the molecular axis, respectively. The value obtained is Ω = 5485(197) ppm. This is a large value, comparable to that obtained for σ. The ^{195}Pt shielding tensor is apparently fairly asymmetric.

7. Conclusions

The pure rotational spectrum of PtCO, generated by ablation of Pt metal in the presence of CO gas, has been measured by FTMW spectroscopy. Because rotational constants have been obtained for several isotopomers, excellent values for the bond lengths have been obtained. These should provide a basis for comparison for ab initio calculations and, indeed, agree fairly well with some recently published values.[4,13] The experimental distortion constants agree well with those calculated from the harmonic force field of Manceron et al.[4] The paramagnetic part and the span of the ^{195}Pt shielding have been evaluated.

Acknowledgment. This work has been supported by the Natural Sciences and Engineering Research Council of Canada (NSERC) and by the Petroleum Research Fund, administered by the American Chemical Society. We thank N. R. Walker for assistance with some of the measurements and R. E. Wasylishen and L. M. Reynard for helpful discussions.

References and Notes

(1) Gottesfeld, S.; Pafford, *J. J. Electrochem. Soc.* **1988**, *135*, 2651.
(2) Dhar, H. P.; Christner, L. G.; Kush, A. K. *J. Electrochem. Soc.* **1987**, *134*, 3021.
(3) Kündig, E. P.; McIntosh, D.; Moskovits, M.; Ozin, G. A. *J. Am. Chem. Soc.* **1973**, *95*, 7234.
(4) Manceron, L.; Tremblay, B.; Alikhani, M. E. *J. Phys. Chem. A* **2000**, *104*, 3750.
(5) Liang, B.; Zhou, M.; Andrews, L. *J. Phys. Chem. A* **2000**, *104*, 3905.
(6) Basch, H.; Cohen, D. *J. Am. Chem. Soc.* **1983**, *105*, 3856.
(7) Basch, H. *Chem. Phys. Lett.* **1985**, *116*, 58.
(8) Rohlfing, C. M.; Hay, P. J. *J. Chem. Phys.* **1985**, *83*, 4641.
(9) Gavezzotti, A.; Tantardini, G. F.; Simonetta, M. *Chem. Phys. Lett.* **1986**, *129*, 577.
(10) Gavezzotti, A.; Tantardini, G. F. *J. Phys. Chem. A* **1988**, *92*, 872.
(11) Smith, G. W.; Carter, E. A. *J. Phys. Chem. A* **1991**, *95*, 2327.
(12) Roszak, S.; Balasubramanian, K. *J. Phys. Chem. A* **1993**, *97*, 11 238.
(13) Chung, S.; Krüger, S.; Ruzankin, S. P.; Pacchioni, G.; Rösch, N. *J. Chem. Phys.* **1995**, *102*, 369.
(14) Chung, S.; Krüger, S.; Pacchioni, G.; Rösch, N. *Chem. Phys. Lett.* **1996**, *109*, 248.
(15) Evans, C. J.; Gerry, M. C. L. *J. Chem. Phys.* **2000**, *112*, 1321.
(16) Evans, C. J.; Gerry, M. C. L. *J. Chem. Phys.* **2000**, *112*, 9363.
(17) Evans, C. J.; Lesarri, A.; Gerry, M. C. L. *J. Am. Chem. Soc.* **2000**, *122*, 6100.
(18) Evans, C. J.; Rubinoff, D.; Gerry, M. C. L. *Phys. Chem. Chem. Phys.* **2000**, *2*, 3943.
(19) Reynard, L. M.; Evans, C. J.; Gerry, M. C. L. *J. Mol. Spectrosc.* **2001**, *206*, 33.
(20) Evans, C. J.; Reynard, L. M.; Gerry, M. C. L. *Inorg. Chem.* **2001**, in press.
(21) Walker, N. R.; Gerry, M. C. L. *Inorg. Chem.* **2001**, in press.
(22) Balle, T. J.; Flygare, W. H. *Rev. Sci. Instrum.* **1981**, *52*, 33.
(23) Xu, Y.; Jäger, W.; Gerry, M. C. L. *J. Mol. Spectrosc.* **1992**, *151*, 206.
(24) Brupbacher, T.; Bohn, R. K.; Jäger, W.; Gerry, M. C. L.; Pasinszki, T.; Westwood, N. P. C. *J. Mol. Spectrosc.* **1997**, *181*, 316.
(25) Walker, K. A.; Gerry, M. C. L. *J. Mol. Spectrosc.* **1997**, *182*, 178.
(26) Pickett, H. M. *J. Mol. Spectrosc.* **1991**, *148*, 371.
(27) Kratzer, A. *Z. Phys.* **1920**, *3*, 289.
(28) Rudolph, H. D. *Struct. Chem.* **1991**, *2*, 581.
(29) Costain, C. C. *J. Chem. Phys.* **1958**, *29*, 864.
(30) Watson, J. K. G.; Roytburg, A.; Ulrich, W. *J. Mol. Spectrosc.* **1999**, *196*, 102.
(31) Kuchitsu, K. *J. Chem. Phys.* **1968**, *49*, 4456.
(32) Kuchitsu, K.; Fukuyama, T.; Morino, Y. *J. Mol. Struct.* **1969**, *4*, 41.
(33) Kuchitsu, K.; Morino, Y. *Bull. Chem. Soc. Jpn.* **1965**, *38*, 805.
(34) Walker, N. R.; Hui, J. K. H.; Gerry, M. C. L., unpublished research, 2001.
(35) Flygare, W. H. *J. Chem. Phys.* **1964**, *41*, 793.
(36) Mills, I.; Cvitaš, T.; Homann, K.; Kallay, N.; Kuchitsu, K. *Quantities, Units and Symbols in Physical Chemistry*, 2nd ed.; Blackwell: Oxford, 1993.
(37) Malli, G.; Fraga, S. *Theor. Chim. Acta* **1966**, *5*, 275.
(38) Wasylishen, R. E.; Bryce, D. L.; Evans, C. J.; Gerry, M. C. L. *J. Mol. Spectrosc.* **2000**, *204*, 184.
(39) Huber, K. P.; Herzberg, G. *Molecular Spectra and Molecular Structure: Constants of Diatomic Molecules*; Van Nostrand: New York, 1979.
(40) Steimle, T. C.; Jung, K. Y.; Li, B. Z. *J. Chem. Phys.* **1995**, *102*, 5937.
(41) Solupe, M.; Bauschlicher, C. W.; Lee, T. J. *Chem. Phys. Lett.* **1992**, *189*, 266.
(42) Kasai, Y.; Obi, K.; Ohshima, Y.; Endo, Y.; Kawaguchi, K. *J. Chem. Phys.* **1995**, *103*, 90.
(43) Zhou, M.; Andrews, L. *J. Phys. Chem. A* **1999**, *103*, 7773.
(44) Tan, H.; Liao, M.; Balasubramanian, K. *Chem. Phys. Lett.* **1998**, *290*, 458.
(45) Zhou, M.; Andrews, L. *J. Phys. Chem. A* **1999**, *103*, 7785.
(46) Zhou, M.; Andrews, L. *J. Am. Chem. Soc.* **2000**, *122*, 1531.